arXiv:1302.4748v1 [cond-mat.supr-con] 19 Feb 2013

First-principles calculations of the improper s-wave symmetry for the electronic pairing in iron-based superconductors

M. Casula*
CNRS and Institut de Minéralogie et de Physique des Milieux condensés,
Université Pierre et Marie Curie, case 115, 4 place Jussieu, 75252, Paris cedex 05, France

S. Sorella†
International School for Advanced Studies (SISSA) Via Beirut 2,4 34014 Trieste,
Italy and INFM Democritos National Simulation Center, Trieste, Italy

(Dated: February 21, 2013)

By means of space-group symmetry arguments, we argue that the electronic pairing in iron-based high temperature superconductors shows a structure which is a linear combination of *planar* s-wave and d-wave symmetry channels, both preserving the 3-dimensional A_{1g} irreducible representation of the corresponding crystal point-group. We demonstrate that the s- and d-wave channels are determined by the parity under reflection of the electronic orbitals through the iron planes, and by improper rotations around the iron sites. We provide evidence of these general properties by performing accurate quantum Monte Carlo ab-initio calculations of the pairing function, for a FeSe lattice with tetragonal experimental geometry at ambient pressure. We find that this picture survives even in the FeSe under pressure and at low temperatures, when the tetragonal point-group symmetry is slightly broken. Our theory can rationalize and explain a series of contradictory experimental findings, such as the observation of twofold symmetry in the FeSe superconducting phase, the anomalous drop of T_c with Co-impurity in LaFeAsO$_{(1-x)}$F$_x$, the s-to-d-wave gap transition in BaFe$_2$As$_2$ under K doping, and the nodes appearing in the LiFeAs superconducting gap upon P isovalent substitution.

PACS numbers: 74.20.-z,74.20.Mn,74.70.Xa,02.70.Ss

The pairing symmetry of the superconducting state in iron-based superconductors (IBS) has been one of the most debated subjects since their first discovery, in both theory and experiments.[1–3] Its determination is particularly challenging in the IBS for their complex electronic structure, with a strong multiband character, and a Fermi surface constituted by many sheets, which can vary with doping and chemical composition. Moreover, the IBS families are usually compensated metals, and thus both electrons and holes are involved in the paired state. Weak-coupling RPA approaches, coupled to multiband BCS theory, yield a pairing function with global s-wave (A_{1g}) symmetry, but with electron and holes pockets having opposite sign. This scenario, dubbed $s^{\pm}$, was first proposed by Mazin *et al.*[4] complemented later with its variants, called "extended $s^{\pm}$",[5] in the case that accidental nodes appear on a single Fermi sheet without breaking the full rotational symmetry. The latest generalizations include also "weak" nodal lines which develop as closed loops on the 3-dimensional (3D) Fermi surface.[6–8]

A variety of experiments has been performed to probe the pairing symmetry of IBS, ranging from thermal conductivity and specific heat measurements to angle-resolved photoemission spectroscopy. While there is no doubt on the spin singlet nature of the pairing state as revealed by the Knight shift,[9] the presence of nodes and the total symmetry of the spatial part of the pairing function are controversial. In fact, the experimental outcome seems to lack universality, as it depends crucially on the "family" of tested compound, its doping, its isovalent substitutions, and its level of disorder. For instance, the situation is paradoxical for the "111" family, where the LiFeAs material shows a fully gapped superconducting order parameter, while the isovalent substitution by phosphorus leads to thermodynamic properties compatible with a nodal pairing function.[10] For the "122" family, there is a recent claim, supported by independent experimental probes, that the pairing in the BaFe$_2$As$_2$ undergoes an s-to-d symmetry change by doping with potassium,[11] the fully substituted KFe$_2$As$_2$ being identified as a d-wave superconductor.[12] In the "1111" family, the dependence of the critical temperature T_c upon disorder has been studied in the LaFeAsO$_{(1-x)}$F$_x$ with $x = 0.11$. It has been found that Co-doping induced disorder makes T_c to fall much more slowly than Mn-doping.[13] This is not compatible with any sign changing order parameter (either $s^{\pm}$ or d-wave). Finally, specific heat measurements performed on the FeSe revealed a highly anisotropic order parameter in the "11" family,[14] with a twofold symmetry directly observed by scanning tunneling microscopy (STM).[15]

In this Letter, we study the IBS gap structure from a different perspective, namely by looking for its *universal* features based on symmetry constraints induced by the 3D *space-group* transformations of the crystals. We prove that the IBS pairing function is a linear combination of terms having planar s- and d-wave symmetries, both fulfilling the full 3D A_{1g} representation. These properties are then verified in the FeSe by performing state-of-the-art quantum Monte Carlo (QMC) calculations from first-principles. Our theory provides a general framework to account for the contradictory experimental outcomes.

The undistorted structure of FeSe, together with the other parent compounds of the "111" and "1111" families, belongs to the $P4/nmm$ space-group, which is nonsymmorphic due to a glide plane parallel to the iron layers. Indeed, its related D_{4h} point-group classes contain certain operations with the nonprimitive lattice translation $\boldsymbol{\tau} = (1/2, 1/2, 0)$ - expressed in crystal units of the 2-Fe unit cell - which brings a Fe site into the other in the cell. This is due to the Se sites alternating above and below the Fe layer. In particular, the C_4 class of pure rotations by $\pi/2$ about the principal axis is not compatible with the 3D lattice, unless associated with the translation $\boldsymbol{\tau}$. On the other hand, the S_4 class, defined as a rotation by $\pi/2$ about the principal axis combined with the reflection σ_h through the Fe plane ($S_4 = C_4\sigma_h$), is a a pure point-group operation allowed by the $P4/nmm$ space-group, as well as the reflection through the plane perpendicular to the Fe (xy) plane and bisecting the secondary (x and y) axes (the σ_d class).

This has important consequences on the symmetries of the subgroup associated with the 2-dimensional (2D) Fe square sublattice, and thus on the low-energy features of the system, as for instance, the superconducting gap structure. Indeed, the standard $C_{4\nu}$ group of the 2D square lattice, generated by the elementary σ_d and C_4 point-group operations, does not fulfill all symmetries of the $P4/nmm$ space-group, whereas the group generated by σ_d and S_4 does. Moreover, proper (C_4) and improper (S_4) rotations differ from the physical point of view, because a Hamiltonian or a pairing function fulfilling the point-group operations generated by S_4 and σ_d will transform in a very different way with respect to those based on the standard $C_{4\nu}$ group, as it will be shown in the following.

From ab-initio electronic structure DFT and DMFT calculations of IBS,[16–18] it is well established that the bands crossing the Fermi level have a strong d-orbital character. Indeed, the minimal tight-binding Hamiltonian which reproduces successfully the Fermi surface contains all the five atomic (or Wannier) d-orbitals centered on the Fe sites,[19] namely $|d_{xz}\rangle$, $|d_{yz}\rangle$, $|d_{xy}\rangle$, $|d_{x^2-y^2}\rangle$, and $|d_{3z^2-r^2}\rangle$, expressed with the crystal axes oriented according to the Fe square lattice directions. A given atomic orbital $d_{\mathbf{R},\nu,\sigma}(\mathbf{r})$ defining the 2D multiorbital model can be represented by $\langle \mathbf{r}|d_{\mathbf{R},\nu,\sigma}\rangle = \langle \mathbf{r}|c^\dagger_{\mathbf{R},\nu,\sigma}|0\rangle$, where $\mathbf{r}$ lives in the 3D space, $\mathbf{R}$ is the center of the atomic orbital on the square lattice, ν is the orbital symmetry, and $\sigma = \pm\frac{1}{2}$ is the electron spin. A spatial point-group operation η acts on the orbital creation operator by changing its position $\mathbf{R} \to R_\eta \mathbf{R}$, its phase $s = 1 \to s'(\eta, \nu) = \pm 1$ and its orbital label $\nu \to \nu'(\eta, \nu)$ according to the general rule:

$$R_\eta c^\dagger_{\mathbf{R},\nu,\sigma} R^\dagger_\eta = c^\dagger_{R_\eta \mathbf{R},\nu,\sigma} = s(\eta,\nu) c^\dagger_{\mathbf{R},\nu'(\eta,\nu),\sigma}. \tag{1}$$

For $\eta = \{\sigma_d, S_4, C_4\}$ and ν given, the corresponding s' and ν' are reported in Tab. I. The transformation rules are different, whether the group is generated by S_4 or C_4.

ν	$\eta = \sigma_d$	$\eta = S_4$	$\eta = C_4$
d_{xz}	$+d_{yz}$	$+d_{yz}$	$-d_{yz}$
d_{yz}	$+d_{xz}$	$-d_{xz}$	$+d_{xz}$
d_{xy}	$+d_{xy}$	$-d_{xy}$	$-d_{xy}$
$d_{x^2-y^2}$	$-d_{x^2-y^2}$	$-d_{x^2-y^2}$	$-d_{x^2-y^2}$
$d_{3z^2-r^2}$	$+d_{3z^2-r^2}$	$+d_{3z^2-r^2}$	$+d_{3z^2-r^2}$

TABLE I: Action of the symmetry operations $\eta = \{\sigma_d, S_4, C_4\}$ on the five iron atomic d-orbitals. The entries represent the pair $s' = \pm$ and $\nu' = d_{xz}, d_{yz}, d_{xy}, d_{x^2-y^2}, d_{3z^2-r^2}$ as a function of the orbital index ν (first column) and the symmetry operation η considered. Note the different s' between proper C_4 and improper S_4 rotations in the first two orbitals (odd with respect to σ_h).

Let us take into account the 2D tight-binding Hamiltonian H_0 which defines the low-energy model for the IBS. It reads as

$$\hat{H}_0 = \sum_{\mathbf{k},\nu,\mu,\sigma} t(\mathbf{k})_{\nu,\mu} c^\dagger_{\mathbf{k},\nu,\sigma} c_{\mathbf{k},\mu,\sigma}, \tag{2}$$

where the vectors $\{\mathbf{k}\}$ belong to the Brillouin zone of the 2D lattice, $c_{\mathbf{k},\nu,\sigma}$ ($c^\dagger_{\mathbf{k},\nu,\sigma}$) is the Fourier transform of $c_{\mathbf{R},\nu,\sigma}$ ($c^\dagger_{\mathbf{R},\nu,\sigma}$), the μ, ν indexes run over the d-orbital labels, the hoppings fulfill the hermitian condition $t(\mathbf{k})^*_{\mu,\nu} = t(\mathbf{k})_{\nu,\mu}$, and $t(-\mathbf{k})_{\nu,\mu} = t(\mathbf{k})^*_{\nu,\mu}$ holds for reality. Obviously, $\hat{H}_0$ must be invariant under the symmetry transformations of the group generated by σ_d and S_4, as the compatible subgroup of the full $P4/nmm$ space-group. If we apply the transformation rules in Eq. 1 to $\hat{H}_0$, and require its invariance, we obtain a set of relations for the hopping matrix:

$$t(R_\eta \mathbf{k})_{\nu,\mu} = s(\eta,\nu) s(\eta,\mu) t(\mathbf{k})_{\nu'(\eta,\nu),\mu'(\eta,\mu)}, \tag{3}$$

for the eight possible independent point-group operations, defined by $\eta = \sigma_d$, S_4, and all their products. These transformations have already been derived in Refs. 20 and 21. However, their implications for the pairing properties have so far been overlooked.

The pairing operator $\hat{F}$ is assumed to be translationally invariant (on the square lattice), so that it is convenient to write it in $\mathbf{k}$-space as

$$\hat{F} = \sum_{\mathbf{k},\nu,\mu} f(\mathbf{k})_{\nu,\mu} c^\dagger_{\mathbf{k},\nu,\uparrow} c^\dagger_{-\mathbf{k},\mu,\downarrow}. \tag{4}$$

Singlet pairing, and no broken time-reversal symmetry imply that $f(\mathbf{k})_{\nu,\mu} = f(-\mathbf{k})_{\mu,\nu}$, and $f(\mathbf{k})_{\nu,\mu} = f(-\mathbf{k})^*_{\nu,\mu}$, respectively. In the following, we derive the spatial-orbital properties of the pairing function $F(\mathbf{r}, \mathbf{r}') = \langle \mathbf{r}, \mathbf{r}'|\hat{F}|0\rangle$, by assuming that it belongs to the A_{1g} irreducible representation of the point-group generated by σ_d and S_4. This assumption will be verified later by ab-initio QMC calculations with a fully optimized Jastrow projected BCS wave function. “Improper s-wave” is the name we assign to the symmetry of the resulting $\hat{F}$, to distinguish it from the standard or “proper” one, i.e. the A_{1g} irreducible representation of the isomorphic point-group where the S_4 class has been replaced by C_4.

Based on the general rules in Eq. 1 and the entries of Tab. I, we can derive the symmetry constraints for the improper s-wave. As the characters of the A_{1g} representation are - by definition - identically one for all classes within the point-group, the symmetry transformations of $f(\mathbf{k})_{\nu,\mu}$ read as

$$f(R_\eta \mathbf{k})_{\nu,\mu} = s(\eta,\nu) s(\eta,\mu) f(\mathbf{k})_{\nu'(\eta,\nu),\mu'(\eta,\mu)}, \tag{5}$$

for $\eta = \sigma_d$, S_4, and all their independent products. The above constraints reduce the variational freedom for the signs of $F(\mathbf{r},\mathbf{r}')$. Accidental nodes must not break the *general* symmetries in Eq. 5. For the improper s-wave, we demonstrate that F has a peculiar, symmetry selected, sign structure. To show this, let us divide the iron d-orbitals into two groups, namely the "even" (e) and"odd" (o) ones, according to their parity under σ_h. The $|d_{xz}\rangle$ and $|d_{yz}\rangle$ orbitals are odd, while $|d_{xy}\rangle$, $|d_{x^2-y^2}\rangle$, and $|d_{3z^2-r^2}\rangle$ are even. Thus, F can be expanded as

$$F = F_{ee} + F_{eo} + F_{oe} + F_{oo}, \tag{6}$$

with its components defined as follows:

$$\begin{aligned}
F_{ee}(\mathbf{r},\mathbf{r}') = &\ \textstyle\sum_{\mathbf{k},\{\nu,\mu\}\in\text{even}} f(\mathbf{k})_{\nu,\mu} d_{\mathbf{k},\nu,\uparrow}(\mathbf{r}) d_{-\mathbf{k},\mu,\downarrow}(\mathbf{r}'),\\
F_{eo}(\mathbf{r},\mathbf{r}') = &\ \sum_{\substack{\mathbf{k},\{\nu\}\in\text{even}\\ \{\mu\}\in\text{odd}}} f(\mathbf{k})_{\nu,\mu} d_{\mathbf{k},\nu,\uparrow}(\mathbf{r}) d_{-\mathbf{k},\mu,\downarrow}(\mathbf{r}'),\\
F_{oe}(\mathbf{r},\mathbf{r}') = &\ \sum_{\substack{\mathbf{k},\{\nu\}\in\text{odd}\\ \{\mu\}\in\text{even}}} f(\mathbf{k})_{\nu,\mu} d_{\mathbf{k},\nu,\uparrow}(\mathbf{r}) d_{-\mathbf{k},\mu,\downarrow}(\mathbf{r}'),\\
F_{oo}(\mathbf{r},\mathbf{r}') = &\ \textstyle\sum_{\mathbf{k},\{\nu,\mu\}\in\text{odd}} f(\mathbf{k})_{\nu,\mu} d_{\mathbf{k},\nu,\uparrow}(\mathbf{r}) d_{-\mathbf{k},\mu,\downarrow}(\mathbf{r}').
\end{aligned}$$

The above pairing functions are periodic in both $\mathbf{r}$ and $\mathbf{r}'$, with periodicity set by the Bravais lattice vectors. In the following analysis, without loss of generality, we are going to pin $\mathbf{r}$ around an iron site[22], while we define $F(k_x,k_y)$ as the 2D Fourier transform of F with respect to the planar (x,y) components of $\mathbf{r}'-\mathbf{r}$. According to the transformation rules in Eq. 5 and in Tab. I, we obtain that F_{ee} and F_{oo} have an s-wave planar symmetry, e.g. $F_{ee}(k_x,k_y) = F_{ee}(-k_x,k_y) = F_{ee}(k_x,-k_y) = F_{ee}(k_y,k_x)$, whereas F_{eo} and F_{oe}, which couple unlike-parity components, have planar d_{xy} symmetry, e.g. $F_{eo}(k_x,k_y) = -F_{eo}(-k_x,k_y) = -F_{eo}(k_x,-k_y) = F_{eo}(k_y,k_x)$. We note here that in a standard s-wave superconductor obeying the $C_{4\nu}$ point-group transformations, also the F_{eo} and F_{oe} components are s-wave. Thus, our improper-s wave pairing function has to have different signs just from symmetry considerations.

These predictions have been verified against accurate ab-initio QMC calculations based on the energy minimization of a Jastrow projected BCS wavefunction, performed for the FeSe on a $4\times4\times1$ iron lattice, subject to periodic boundary conditions. We used the experimental FeSe geometry, determined at ambient pressure (0 GPa) and temperature[23] and under a hydrostatic pressure of 4 GPa at low-temperature.[24] Fe and Se atoms have been replaced by pseudoatoms, containing only 16 and 6 valence electrons, respectively.[25] The full many-body wave function can be written in a compact form as $\Psi_{\text{JBCS}}(\mathbf{R}_{\text{el}}) = \exp[-J(\mathbf{R}_{\text{el}})]\det[\phi(\mathbf{r}_i^{\uparrow},\mathbf{r}_j^{\downarrow})]$, where $1\le i,j\le N/2$, with N the total number of electrons in the supercell, and $\mathbf{R}_{\text{el}} = \{\mathbf{r}_1^{\uparrow},\ldots,\mathbf{r}_{N/2}^{\uparrow},\mathbf{r}_1^{\downarrow},\ldots,\mathbf{r}_{N/2}^{\downarrow}\}$ the many-body electron configuration. Dynamic correlations, including charge fluctuations, are taken into account by the Jastrow factor J, while correlations built up in the superconducting state are described by the BCS pairing function ϕ, which reads as

$$\phi(\mathbf{r},\mathbf{r}') = \sum_{i=1}^{M} \lambda_i \psi_i^{MO}(\mathbf{r}) \psi_i^{MO}(\mathbf{r}'). \tag{7}$$

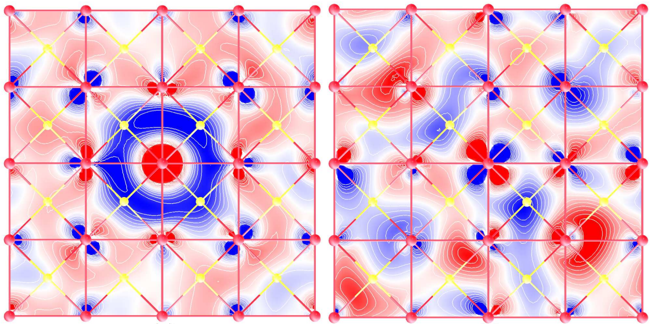
(a) (b)

FIG. 1: Even-even (panel a), and odd-even (panel b) components of the pairing function ϕ^{corr} of the FeSe high-T$_c$ superconductor at 0 GPa obtained by QMC, by optimizing the energy of the variational wavefunction without assuming any global symmetry. The contour plots show $\phi^{corr}(\mathbf{R}_{\text{center}},\mathbf{r})$ with $\mathbf{R}_{\text{center}}$ set to be the iron lattice site at the center of the supercell, while $\mathbf{r}$ spans the plane defined by the 4×4 lattice. Red (yellow) balls are iron (selenium) sites. Arbitrary units blue (red) intensity indicates negative (positive) regions with corresponding magnitude.

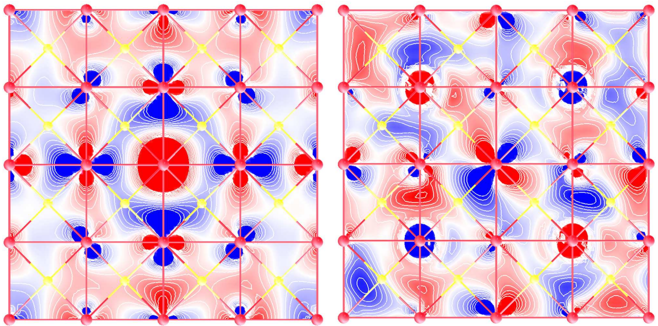
(a) (b)

FIG. 2: The same as in Fig. 1 but for a structure corresponding to a pressure of 4 GPa.

The above expansion is on the lowest M molecular orbitals (MO) ψ_i^{MO}, generated by density functional theory (DFT) calculations, and further optimized by QMC[25]. In all the calculations quantum effects on nuclei are neglected, within the Born-Oppenheimer approximation. Hence superconductivity is assumed to be non conventional, namely not coming from electron-phonon coupling.

$\phi(\mathbf{r},\mathbf{r}')$ is an extension of $F(\mathbf{r},\mathbf{r}')$ in Eq. 6, as it is expanded over the full atomic basis set used to represent the MO's. The resulting ϕ, restricted to its correlated part ϕ^{corr} (obtained by summing the MOs in Eq. 7 over i with $N/2 < i \le M$), is plotted in Figs. 1 and 2 for 0 and 4 GPa, respectively. ϕ^{corr} has been projected over its 4 possible components ϕ^{corr}_{ee} (Figs. 1(a) and 2(a)), ϕ^{corr}_{oo}, ϕ^{corr}_{eo}, and ϕ^{corr}_{oe} (Figs. 1(b) and 2(b)), based on the parity with respect to σ_h [26]. The final picture is remarkably consistent with the improper s-wave pairing function predicted by the 2D point-group symmetries and under the assumption of a 3D A_{1g} irreducible representation. Our QMC solution is A_{1g} as a consequence of an unbiased energy minimization, and it has not been imposed a priori in the optimization. Thanks to the improper S_4 generated point-group, the pairing function ϕ shows two planar symmetry channels, s-wave for the ϕ_{ee}^{corr} and ϕ_{oo}^{corr}, d$_{xy}$-wave for the ϕ_{eo}^{corr} and ϕ_{oe}^{corr} components. We emphasize that ϕ does not possess a well defined symmetry under a proper rotation by $\pi/2$, just because such a rotation is not a symmetry of the crystal. Moreover, Fig. 2 shows that this picture holds even when the tetragonal point-group symmetry is slightly broken, and lowered to the orthorhombic point-group, as in the case of applied pressure and/or low temperature.

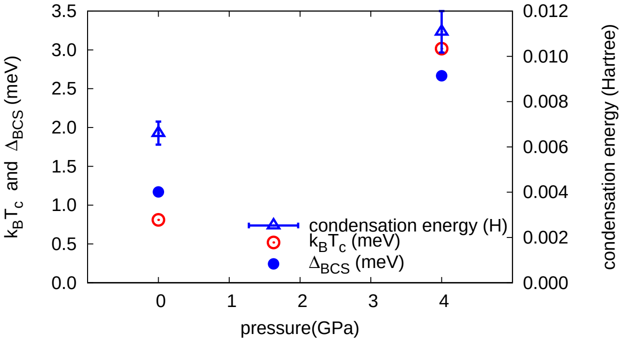

FIG. 3: Condensation energy in the $4x4$ system (in Hartree), and pairing gap Δ_{BCS} (in meV) at 0 and 4 GPa, obtained from our QMC calculations, compared to the experimental superconducting temperature T$_c$ in meV.

To further check the reliability of $\Psi_{\rm JBCS}$ to describe the superconducting features of FeSe, we estimated (via correlated sampling) the condensation energy ϵ_{cond}, defined as the difference between the expectation value of H computed with the fully paired $\Psi_{\rm JBCS}$ and the one with the Jastrow projected single determinant, obtained by summing the MOs with $i \leq N/2$ in Eq. 7. Another independent test has been done by fitting the variational parameters λ_i in Eq. 7 for $i > N/2$ with the BCS expression $\Delta_{BCS}/(\epsilon_i - \mu + \sqrt{(\epsilon_i-\mu)^2 + \Delta_{BCS}^2})$, where we took $\epsilon_i = \epsilon_i^{DFT}$ (the DFT energy of the corresponding MO), μ equal to the Fermi level, and Δ_{BCS} the only fitting parameter. Those quantities are much more sensitive to finite size errors than the pairing symmetry, set by the short-range behavior of ϕ, which is converged in the 4×4 supercell. The ϵ_{cond} and Δ_{BCS} are shown in Fig. 3, together with the experimental critical temperature T_c. It turns out that $\Delta_{BCS} \approx T_c$, which is a remarkable result given the tiny energy scale (of the order of 1 meV) involved in the gap opening. Both ϵ_{cond} and Δ_{BCS} follow quite well the behavior of the experimental T_c, which increases with pressure, in the pressure range considered here[27]. Therefore, our pairing function describes reasonably well the experiments. Remarkably, we are close to make quantitative predictions on unconventional high temperature superconductors by means of a fully ab-initio method.

We explore now the physical consequences of the improper s-wave from a general perspective, by assuming that also the other IBS families have a A_{1g} superconducting gap, as the FeSe. First of all, the twofold symmetry of the pairing function observed by STM[15] in stoichiometric FeSe with impurities and magnetic field can be explained by assuming that the interference states probed by the STM tip are affected by the sign change induced by a planar superposition of the s- and d-wave channels, invariant under π rotations. Note that there are two possible arrangements, oriented in a d$_{xy}$ fashion and tilted by $\pi/2$, in agreement with the different orientations measured by the STM zero bias conductance.

From ab-initio DFT and DMFT calculations,[17, 18] the $d_{x^2-y^2}$ and $d_{3z^2-r^2}$ orbitals are usually pseudogapped. This allows us to disregard them from the summation in Eq. 4. Thus, d_{xy} is the only remaining orbital with even parity, and it can trigger the formation of the d-wave channel in the pairing function. Indeed, for absent or weak d_{xy} spectral weight at the Fermi level, the two orbitals left in F are both odd under σ_h, and therefore they can only contribute to the s-wave channel.

In the "111" family, DFT band structure calculations and de Haas-van Alphen experiments show that the main effect of P isovalent substitution is the formation of the third hole pocket - with dominant d_{xy} character -, absent in the LiFeAs.[28] The enhanced d_{xy} spectral weight in the P substituted compound and the subsequent development of an "even-odd" d-wave pairing gap can explain why the LiFeP pairing is nodal, while the LiFeAs shows a fully gapped behavior.

Within the improper s-wave picture, the properties of the "1111" family modified by impurity substitution as in Ref. 13 are consistent with a tendency of F to develop nodes by going from Co to Mn doping through the opening of the d-wave channel. Indeed, Co impurities are electron donors, while Mn impurities dope the system with hole, thus enhancing the d_{xy} spectral weight around Γ.

The "122" family does not belong to the $P4/nmm$ space-group. Nevertheless, by inspection of its $I4/mmm$ space-group unit cell, one can see that also in that case the S_4 improper rotation is the valid symmetry on the iron layer, thus the improper s-wave theory applies also here. The s-to-d wave transition by doping the BaFe$_2$As$_2$ with K is one of the most striking experimental situations for us.[11] In the strong overdoped regime, the band structure certainly shows all three pockets at Γ with again an enhanced d_{xy} spectral weight. If the d-wave channel dominates in the improper s-wave gap, then it is plausible that the experimental thermodynamic features are compatible with a pure d-wave behavior.

Finally, we would like to point out that the importance of the third hole pocket, with strong d_{xy} character, has already been observed by Kuroki and co-workers in relation to the T_c dependence on the pnictogen height.[29] The improper s-wave symmetry explains the key role played by d_{xy}, particularly in connection with the appearance of gap nodes, the twofold anisotropy, and the stabilization of the d-wave channel, by reconciling a series of experiments which look otherwise contradictory. It suggests also that the pnictogen or the chalcogen, rather than being spectators, take an active role in the electronic pairing, by bridging two next-nearest neighbor iron sites in a d_{xy} fashion via the improper s-wave symmetry.

We acknowledge useful discussions with S. Biermann, T.

Cren, M. Fabrizio, A. Savin, and D. J. Scalapino. The HPC resources have been provided under the IDRIS/GENCI 2012096493 and CINECA-MIUR ISCRA-HP10A2GZHV grants.

---

[*] michele.casula@impmc.upmc.fr

[†] sorella@sissa.it

[1] J. Paglione, and R. L. Greene, Nature Phys. **6**, 645 (2010).

[2] G. R. Stewart, Rev. Mod. Phys. **83**, 1589 (2011).

[3] P. J. Hirschfeld, M. M. KOrshunov, and I. I. Mazin, Rep. Prog. Phys. **74** 124508 (2011).

[4] I. I. Mazin, D. J. Singh, M. D. Johannes, and M. H. Du, Phys. Rev. Lett. **101**, 057003 (2008).

[5] K. Kuroki, S. Onari, R. Arita, H. Usui, Y. Tanaka, H. Kontani, and H. Aoki, Phys. Rev. Lett. **101**, 087004 (2008).

[6] S. Graser, A. F. Kemper, T. A. Maier, H. P. Cheng, P. J. Hirschfeld, and D. J. Scalapino, Phys. Rev. B **81**, 214503 (2010).

[7] K. Suzuki, H. Usui, and K. Kuroki, J.Phys.Soc.Japan **80**, 013710 (2011).

[8] I. I. Mazin, T. P. Devereaux, J. G. Analytis, J.-H. Chu, I. R. Fisher, B. Muschler, and R. Hackl, Phys. Rev. B **82**, 180502(R) (2010).

[9] F. Ning, K. Ahilan, T. Imai, A. S. Sefat, R. Jin, M. A. McGuire, B. C. Sales, and D. Mandrus, J. Phys. Soc. Japan **77**, 103705 (2008).

[10] K. Hashimoto, S. Kasahara, R. Katsumata, Y. Mizukami, M. Yamashita, H. Ikeda, T. Terashima, A. Carrington, Y. Matsuda, T. Shibauchi, Phys. Rev. Lett. **108**, 047003 (2012).

[11] J-Ph. Reid, A. Juneau-Fecteau, R. T. Gordon, S. René de Cotret, N. Doiron-Leyraud, X. G. Luo, H. Shakeripour, J. Chang, M. A. Tanatar, H. Kim, R. Prozorov, T. Saito, H. Fukazawa, Y. Kohori, K. Kihou, C. H. Lee, A. Iyo, H. Eisaki, B. Shen, H-H. Wen, and L. Taillefer, Supercond. Sci. Technol. **25**, 084013 (2012).

[12] J. K. Dong, S. Y. Zhou, T. Y. Guan, H. Zhang, Y. F. Dai, X. Qiu, X. F. Wang, Y. He, X. H. Chen, S. Y. Li, Phys. Rev. Lett. **104**, 087005 (2010).

[13] M. Sato, Y. Kobayashi, S. C. Lee, H. Takahashi, E. Satomi, and Y. Miura J. Phys. Soc. Jap. **79**, 014710 (2010).

[14] B. Zeng, G. Mu, H. Q. Luo, T. Xiang, I. I. Mazin, H. Yang, L. Shan, C. Ren, P. C. Dai, H.-H. Wen, Nature Communications **1**, 112 (2010).

[15] C.-L. Song, Y.-L. Wang, P. Cheng,Y.-P. Jiang, W. Li, T. Zhang, Z. Li, K. He, L. Wang, J.-F. Jia, H.-H. Hung, C. Wu, X. Ma, X. Chen, Q.-K. Xue, Science **332**, 1410 (2011).

[16] D. J. Singh and M.-H. Du, Phys. Rev. Lett. **100**, 237003 (2008).

[17] M. Aichhorn, S. Biermann, T. Miyake, A. Georges, and M. Imada, Phys. Rev. B **82**, 064504 (2010).

[18] Ph. Werner, M. Casula, T. Miyake, F. Aryasetiawan, A. J. Millis, and S. Biermann, Nature Physics **8**, 331 (2012).

[19] S. Graser, T. A. Maier, P. J. Hirschfeld, and D. J. Scalapino, New J. Phys. **11**, 025016 (2009).

[20] K. Nakamura, R. Arita, and M. Imada, J. Phys. Soc. Jpn. **77**, 093711 (2008).

[21] T. Miyake, K. Nakamura, R. Arita, and M. Imada, J. Phys. Soc. Jpn. **79**, 044705 (2010).

[22] Strictly speaking, the d orbitals are zero at the iron sites. The amplitude of the pairing function is computed by integrating those orbitals over a planar mesh ($+\delta_x, -\delta_x, +\delta_y, -\delta_y$, with $|\delta| = 0.25$ Bohr) around the iron center. The sign of the integrand on the mesh selects their angular symmetry.

[23] R. S. Kumar, Y. Zhang, S. Sinogeikin, Y. Xiao, S. Kumar, P. Chow, A. L. Cornelius, and C. Chen, J. Phys. Chem. B **114**, 12597 (2010).

[24] S. Margadonna, Y. Takabayashi, Y. Ohishi, Y. Mizuguchi, Y. Takano, T. Kagayama, T. Nakagawa, M. Takata, and K. Prassides, Phys. Rev. B **80**, 064506 (2009).

[25] See the Supplemental Material for a description of the QMC methods used in this work.

[26] The parity projection has been made by averaging the orbitals at opposite positions above and below the iron layer at a given distance δ_z from it (0.25 Bohr). The odd orbitals are strictly zero at the iron layer. However, the pairing function is 3D. Averaging those orbitals above and below the layer gives a finite contribution. Therefore, the even and odd MO orbitals entering the pairing function ϕ in Eq. 7 read as:

$$
\begin{aligned}
\psi_i^{MO\,\text{odd}}(\mathbf{r}) &= 1/2(\psi_i^{MO}(\mathbf{r}+\delta_z) - \psi_i^{MO}(\mathbf{r}-\delta_z)),\\
\psi_i^{MO\,\text{even}}(\mathbf{r}) &= 1/2(\psi_i^{MO}(\mathbf{r}+\delta_z) + \psi_i^{MO}(\mathbf{r}-\delta_z)).
\end{aligned}
$$

[27] At ambient pressure, the slightly broken low temperature phase is very close to the tetragonal parent structure, and their difference (around 0.01Å between the a and b axes) has been neglected in our calculations. At 4 GPa, the a/b anisotropy is instead more than four times stronger, and thus we used the corresponding experimental low temperature orthorombic structure.

[28] C. Putzke, A. I. Coldea, I. Guillamn, D. Vignolles, A. McCollam, D. LeBoeuf, M. D. Watson, I. I. Mazin, S. Kasahara, T. Terashima, T. Shibauchi, Y. Matsuda, and A. Carrington, Phys. Rev. Lett. **108**, 047002 (2012).

[29] K. Kuroki, H. Usui, S. Onari, R. Arita, and H. Aoki, Phys. Rev. B **79**, 224511 (2009).